Cancer Therapy: Preclinical

Clinical Cancer Research

Carfilzomib and ONX 0912 Inhibit Cell Survival and Tumor Growth of Head and Neck Cancer and Their Activities Are Enhanced by Suppression of Mcl-1 or Autophagy

Yan Zang[1], Sufi M. Thomas[2,3], Elena T. Chan[4], Christopher J. Kirk[4], Maria L. Freilino[2], Hannah M. DeLancey[1], Jennifer R. Grandis[2,3], Changyou Li[1], and Daniel E. Johnson[1,3]

Abstract

Purpose: Carfilzomib is a selective, irreversible inhibitor of the chymotrypsin-like activity of the proteasome and is undergoing clinical evaluation in myeloma. ONX 0912 (oprozomib) is an orally bioavailable derivative. The activities of carfilzomib and ONX 0912 against solid tumor malignancies are less well understood. We investigated the impact and mechanisms of action of carfilzomib and ONX 0912 in preclinical models of head and neck squamous cell carcinoma (HNSCC).

Experimental Design: The effects of carfilzomib and ONX 0912 on HNSCC cell survival and xenograft tumor growth were evaluated. The impact and mechanisms of both agents on apoptosis and autophagy induction were also investigated. The contribution of the unfolded protein response (UPR) to autophagy induction and the role of autophagy in attenuating HNSCC cell death were determined.

Results: Carfilzomib and ONX 0912 potently induced apoptosis in HNSCC cell lines via upregulation of pro-apoptotic Bik. Upregulation of Mcl-1 by these agents served to dampen their efficacies. Carfilzomib and ONX 0912 also induced autophagy, mediated, in part, by activation of the UPR pathway involving upregulation of ATF4 transcription factor. Autophagy induction served a prosurvival role. Oral administration of ONX 0912 inhibited the growth of HNSCC xenograft tumors in a dose-dependent manner.

Conclusions: These results show that carfilzomib and ONX 0912 are potently active against HNSCC cells, and the activities of these agents can be enhanced via suppression of Mcl-1 or inhibition of autophagy. Oral ONX 0912 exhibits *in vivo* activity against HNSCC tumors and may represent a useful therapeutic agent for this malignancy. *Clin Cancer Res; 18(20); 5639–49. ©2012 AACR.*

Introduction

The proteasome plays an important role in regulating cell growth by promoting ubiquitin-mediated degradation of proteins that regulate cellular proliferation and survival (1). Pharmacologic inhibition of the proteasome is emerging as a promising anti-cancer strategy. The 26S constitutive proteasome complex expressed in most cell types contains a 20S catalytic core with chymotrypsin-like (CT-L), caspase-like (C-L), and trypsin-like (T-L) activities (2, 3). *In vitro* and *in vivo* studies have shown that the CT-L activity is rate limiting for proteolysis by the proteasome (3–5). Bortezomib is a first-in-class compound that reversibly inhibits both the CT-L and C-L activities of the proteasome and has been approved by the U.S. Food and Drug Administration (FDA) for use in multiple myeloma and mantle cell lymphoma (6–9). Clinical application of bortezomib is limited by *de novo* and acquired resistance, as well as adverse toxicities (7, 8, 10–13). Development of peripheral neuropathy has been estimated at 35% to 52% in patients with bortezomib-treated myeloma (10, 12, 14, 15), with recent studies suggesting this may be due to off-target inhibition of cellular serine proteases, including cathepsins A and G, chymase, dipeptidyl peptidase II, and HtrA2/Omi (16).

Carfilzomib, a next-generation irreversible proteasome inhibitor, is a tetrapeptide epoxyketone compound that displays a high degree of selectivity for the CT-L activity of the proteasome (17, 18). Carfilzomib is well-tolerated in both mice and humans (18, 19) and displays antitumor activity against lymphoma, myeloma, and Waldenstrom macroglobulinemia (17, 18, 20). Notably, carfilzomib shows activity against myeloma cells resistant to bortezomib, melphalan, and dexamethasone (17). Synergism of carfilzomib with dexamethasone or histone deacetylase inhibitors has been reported (17, 21). In contrast to bortezomib, carfilzomib fails to inhibit the C-L activity of the

Authors' Affiliations: Departments of [1]Medicine, [2]Otolaryngology, and [3]Pharmacology & Chemical Biology, University of Pittsburgh, University of Pittsburgh Cancer Institute, Pittsburgh, Pennsylvania; and [4]Research, Onyx Pharmaceuticals, Inc., South San Francisco, California

Note: Supplementary data for this article are available at Clinical Cancer Research Online (http://clincancerres.aacrjournals.org/).

Corresponding Author: Daniel E. Johnson, University of Pittsburgh School of Medicine, Room 2.18c, Hillman Cancer Center, 5117 Centre Avenue, Pittsburgh, PA 15213. Phone: 412-623-3245; Fax: 412-623-7768; E-mail: johnsond@pitt.edu

doi: 10.1158/1078-0432.CCR-12-1213

Translational Relevance

Application of the reversible proteasome inhibitor bortezomib to solid tumors is hindered by the need for frequent dosing, development of peripheral neuropathy, and drug resistance. Carfilzomib, a second-in-class proteasome inhibitor, is a highly selective, irreversible inhibitor of the chymotrypsin-like activity of the proteasome and is associated with reduced peripheral neuropathy. The derivative compound, ONX 0912, offers a further advantage of being orally bioavailable.

We show that carfilzomib and ONX 0912 potently kill head and neck squamous cell carcinoma (HNSCC) cells via upregulation of Bik. Oral administration of ONX 0912 markedly reduced the growth of HNSCC tumors *in vivo*. Our mechanistic studies reveal that both compounds also induce anti-apoptotic Mcl-1 and prosurvival autophagy. Suppression of Mcl-1 or autophagy enhanced the killing activities of carfilzomib and ONX 0912, providing a strategy for further improving the efficacies of these promising proteasome inhibitors against HNSCCs.

proteasome or other serine protease targets of bortezomib (16). The greater selectivity of carfilzomib may explain the low rates of peripheral neuropathy observed in early-phase clinical trials with this agent.

Bortezomib and carfilzomib require intravenous or subcutaneous administration. In contrast, ONX 0912, a recently generated derivative of carfilzomib, is orally bioavailable (22). Similar to carfilzomib, ONX 0912 promotes cell death in myeloma cells from patients who relapsed after treatment with bortezomib, dexamethasone, or lenalidomide (23). ONX 0912 antitumor activity has been shown in myeloma and lymphoma xenograft models (22, 23). The ability to deliver ONX 0912 via oral administration, coupled with activity against tumor cells resistant to bortezomib or other conventional therapies, has heightened interest in this novel proteasome inhibitor.

While the antitumor activities of carfilzomib and ONX 0912 against a variety of hematologic malignancies have been reported, considerably less is known about their effects on solid tumors, including head and neck squamous cell carcinoma (HNSCC). HNSCC is a common cancer, with 5-year survival rates that have lingered around 50% for the past several decades (24). Despite FDA approval in 2006, cetuximab treatment benefits only a small percentage of patients with HNSCCs (25), and the current therapeutic approaches of surgery, radiation, and chemotherapy are associated with considerable adverse toxicities, deficits in speaking and swallowing, and disfigurement. Thus, there is a compelling need to develop new and effective therapeutic agents and strategies for this malignancy. Bortezomib has been reported to promote HNSCC cell death both *in vitro* and *in vivo* (26–29). Moreover, the combination of bortezomib with radiation in recurrent HNSCCs showed sustained partial responses in 5 of 18 patients and temporary responses or disease stabilization in additional patients (30, 31). In view of the greater selectivities of carfilzomib and ONX 0912 and the oral bioavailability of ONX 0912, we sought to determine the activities and mechanisms of action of these compounds against HNSCCs *in vitro* and *in vivo*.

We report that carfilzomib and ONX 0912 potently promote cell death in 8 different HNSCC cell lines. Induction of cell death was associated with activation of apoptosis signaling, as assessed by caspase activation and Annexin V staining. Treatment with either agent resulted in upregulation of pro-apoptotic Bik as well as anti-apoptotic Mcl-1. Prevention of Bik or Mcl-1 upregulation by siRNAs revealed that Bik mediates, whereas Mcl-1 attenuates, carfilzomib- and ONX 0912–induced HNSCC cell death. Both agents also induced autophagy, associated with upregulation of Beclin-1, Atg5/12 conjugate, and LC3-II, and formation of autophagosomes. Complete autophagic flux was shown in studies incorporating inhibitors of lysosomal proteases. Importantly, inhibition of autophagy enhanced proteasome inhibitor–induced cell death. Autophagy induction was preceded by activation of the unfolded protein response (UPR), resulting in elevated levels of phospho-PKR-like endoplasmic reticulum kinase (PERK), phospho-eIF2α, and ATF4 transcription factor. Carfilzomib- and ONX 0912–induced autophagy was partially dependent on ATF4. Finally, oral administration of ONX 0912 was found to significantly inhibit the growth of HNSCC xenograft tumors. These findings provide the basis for clinical testing of carfilzomib and ONX 0912 in HNSCCs and suggest that the impact of these agents may be enhanced by combining with inhibitors of Mcl-1 or autophagy.

Materials and Methods

Cells and reagents

The human HNSCC cell lines UMSCC-22A, UMSCC-22B, 1483, UMSCC-1, and Cal33 (32) were grown at 37°C in Dulbecco's Modified Eagles' Media (DMEM) containing 10% heat-inactivated FBS (HyClone Laboratories), 100 units/mL penicillin, and 100 μg/mL streptomycin (Invitrogen). UMSCC-22A cells stably expressing GFP-LC3 (33) were maintained in medium containing 500 μg/mL G418 (Mediatech). All cell lines were genotypically validated using the AmpFlSTR Profiler Plus Kit from PE Biosystems, according to the manufacturer's instructions. E64d, pepstatin A, leupeptin, and chloroquine were from Sigma.

Cell viability and apoptosis assays

Cell viabilities were assessed by trypan blue exclusion assays. Briefly, cells were seeded in triplicate at 2.0×10^4 to 2.5×10^4 cells per well in 48-well plates, allowed to grow overnight, and then treated for 48 hours with carfilzomib or ONX 0912. Control cells were treated with 0.1% dimethyl sulfoxide (DMSO), the drug diluent. Following treatment, floating cells were combined with trypsinized cells, and viabilities were determined by counting a minimum of 300 cells per data point. IC_{50} values were determined using

GraphPad Prism software (GraphPad Software, Inc.). Apoptosis was quantified by conducting Annexin V/propidium iodide (PI) staining (BD BioScience, Inc.), followed by two-color flow cytometric analysis using an Epics Coulter XL flow cytometer (Beckman Coulter).

Immunoblotting

Immunoblotting used antibodies directed against Bcl-X_L (cat. #sc-8392), Mcl-1 (sc-819), Bik (sc-10770), Bax (sc-493), Beclin-1 (sc-11427), total PERK (sc-13073), and ATF4 (sc-200) from Santa Cruz Biotechnology, Inc.; Bcl-2 (M0887; Dako Corp.); Bim (AAP-330) and caspase-3 (AAP-113) from Assay Designs; Bak (3814), PARP (9542), and phospho-eIF2α (3597; Ser51) from Cell Signaling Technology; LC3 (NB100-2220) and Atg5/12 (NB110-53818) from Novus Biologicals, Inc.; total eIF2α (606702) and phospho-PERK (649402; Ser713) from BioLegend; and β-actin (A5441) from Sigma.

siRNA transfection

Cells were seeded at 6.5×10^5 cells per plate in 60-mm dishes and grown overnight. The medium was then replaced with DMEM lacking serum and antibiotics. Annealed siRNAs were diluted to 100 nmol/L in Opti-Mem (Gibco Life Technologies) and then transfected into cells using Lipofectamine 2000 (Invitrogen) following the manufacturer's instructions. After 6 hours, the medium was replaced with fresh DMEM containing 10% FBS and antibiotics, and incubation continued for an additional 18 hours before treatment with the proteasome inhibitors. Nonspecific siRNA was from Ambion, as were siRNAs for Mcl-1 (5′-CCAGUAUACUUCUUAGAAATT-3′), Bik (5′-GGGAUGUUCUUAGAAGUUUTT-3′), and ATF4 (5′-GCCUAGGUCUCUUAGAUGATT-3′).

Detection and quantification of GFP-LC3 puncta

UMSCC-22A cells stably expressing GFP-LC3 (33) were seeded at 6.5×10^4 cells per well on microscope coverslips in 24-well plates and grown overnight. Following treatment, cells were fixed in 4% paraformaldehyde, rinsed twice with cold PBS, and briefly dried. The fixed cells were stained with Hoechst 33258 (Sigma) and then rinsed 3 times with PBS. After drying, the cells were sealed with mounting medium. Images detecting GFP-LC3 punctate dots were captured using a confocal Olympus Flueview 1000 microscope. For each treatment condition, the average number of GFP-LC3 puncta per cell was determined by counting 5 random fields, with a minimum of 25 cells per field. The graphed data represents the mean number of puncta per cell from 3 independent experiments.

In vivo inhibition CT-L activities and tumor growth

All animal studies were approved by the University of Pittsburgh Institutional Animal Care and Use Committee (Pittsburgh, PA). Athymic nude mice were inoculated subcutaneously in the flank with the HNSCC cell line Cal33 (0.5×10^6 cells). Mice bearing tumors between 3 and 5 mm in diameter were randomized into 3 groups of 3 mice per group for assessment of *in vivo* CT-L activities or 10 mice per group for tumor growth studies. CT-L activities in normal and tumor tissues were determined as previously described (18). For tumor growth studies, tumors were measured twice weekly in 2 perpendicular dimensions using vernier calipers. Animals were treated via oral gavage with vehicle control (1% carboxymethyl cellulose in 0.2 mL saline) or ONX 0912 (10 or 30 mg/kg body weight in 0.2 mL).

Statistical analysis

For *in vitro* studies, the statistical significance of differences between 2 groups was determined by one-way ANOVA. For *in vivo* studies, 2-way comparisons between tumor volumes of mice treated with vehicle or ONX 0912 were carried out using the Kruskal–Wallis exact test for K-independent samples with StatXact-9 (Cytel Studio) software. *P* values less than 0.05 were considered statistically significant.

Results

Carfilzomib and ONX 0912 induce apoptosis signaling and cell death in HNSCC cells

To investigate the activities of carfilzomib and ONX 0912 against HNSCCs, we used 8 different cell lines (Table 1). The HNSCCs were treated for 48 hours with varying concentrations of carfilzomib or ONX 0912, followed by performance of trypan blue exclusion assays. The IC_{50} values presented in Table 1 represent the average of values obtained in 3 independent experiments (raw data are shown in Supplementary Fig. S1A and S1B). Carfilzomib exhibited IC_{50} values ranging from 18.3 to 70.4 nmol/L in the 8 different cell lines. ONX 0912 was somewhat less potent, with IC_{50} values ranging from 58.9 to 185.7 nmol/L. The roughly 3-fold lower potency of ONX 0912, relative to carfilzomib, was consistent with prior demonstration that ONX 0912 is somewhat less potent than carfilzomib at inhibiting the CT-L activity of the proteasome (22). We then examined the impact of carfilzomib and ONX 0912 on cellular apoptosis using 4 HNSCC cell lines (UMSCC-1, UMSCC-22B, 1483, and UMSCC-1) which have been extensively characterized with respect to molecular mechanisms of proliferation and survival and responsiveness to molecular targeting agents.

Table 1. IC_{50} values (nmol/L) of carfilzomib and ONX 0912 against HNSCC cell lines

	Carfilzomib	ONX 0912
UMSCC-22A	38.7 ± 1.0	98.5 ± 10.3
UMSCC-22B	30.7 ± 9.3	106.5 ± 9.7
1483	50.5 ± 11.9	152.0 ± 20.5
UMSCC-1	34.6 ± 2.6	135.8 ± 15.6
Cal33	49.3 ± 8.9	88.5 ± 1.4
PCI-15A	70.4 ± 22.6	185.7 ± 7.1
PCI-15B	39.5 ± 11.0	105.7 ± 3.4
OSC-19	18.3 ± 4.2	58.9 ± 8.8

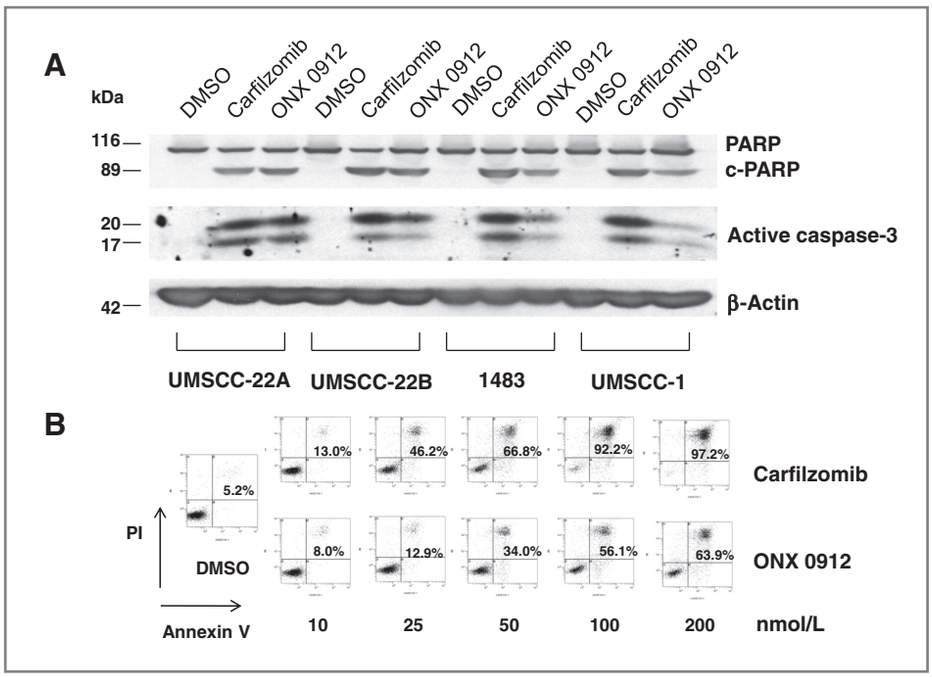

Figure 1. Carfilzomib and ONX 0912 induce apoptosis signaling in HNSCCs. A, UMSCC-22A, UMSCC-22B, 1483, and UMSCC-1 cells were treated for 24 hours with 0.1% DMSO or 200 nmol/L carfilzomib or ONX 0912, followed by immunoblotting with anti-PARP, anti-caspase-3, or anti-β-actin. Shown are full-length PARP, cleaved PARP (c-PARP), and the cleaved, active subunits of caspase-3. Similar results were obtained in 3 independent experiments. B, UMSCC-22A cells were treated for 48 hours with 0.1% DMSO or varying concentrations of carfilzomib or ONX 0912, followed by flow cytometric analysis of Annexin V/PI staining. Numbers indicate the percentage of Annexin V–positive cells. The experiment was carried out 3 times with similar results.

Treatment of HNSCCs with carfilzomib or ONX 0912 led to the activation of apoptosis signaling. In the 4 HNSCC cell lines examined, treatment resulted in processing of caspase-3 to active subunits and cleavage of the caspase substrate PARP (Fig. 1A). Flow cytometric detection of Annexin V staining confirmed the activation of HNSCC cell apoptosis (Fig. 1B).

To further assess the importance of caspase-3 activation, UMSCC-22A and 1483 cells were treated with carfilzomib or ONX 0912 in the absence or presence of the caspase-3 inhibitor z-DEVD or the pan-caspase inhibitor z-VAD (Supplementary Fig. S2A and S2B). Treatment with either inhibitor partially inhibited carfilzomib- and ONX 0912–induced apoptosis as determined by Annexin V staining. Thus, induction of HNSCC apoptosis by these proteasome inhibitors is at least partially dependent on caspase-3.

Bik mediates and Mcl-1 attenuates carfilzomib- and ONX 0912–induced HNSCC apoptosis

The proteasome regulates the expression levels of multiple proteins involved in cellular proliferation and survival, including several members of the Bcl-2 protein family. Thus, we next investigated the impact of carfilzomib and ONX 0912 on the expression of Bcl-2 family members (Fig. 2A). Both upregulation and downregulation of Bcl-2 family members were observed, with similar trends in all 4 HNSCC cell lines, and similar results with both agents. Marked downregulation of anti-apoptotic Bcl-2 was observed in the 3 cell lines that expressed this protein. In contrast, anti-apoptotic Bcl-X_L and Mcl-1 were upregulated in all 4 cell lines, with Mcl-1 upregulation being particularly dramatic. With respect to pro-apoptotic proteins, strong upregulation of Bik was seen in 2 cell lines and more modest upregulation was seen in the other 2 lines. Modest upregulation of Bim and Bax was detected in all 4 lines. The expression of Bak did not appear to be appreciably altered.

In view of the strong upregulation of pro-apoptotic Bik and anti-apoptotic Mcl-1, we sought to determine the significance of these events for carfilzomib- and ONX 0912–induced HNSCC apoptosis. Upregulation of Bik and Mcl-1 was prevented by treating UMSCC-22A (Fig. 2B), 1483 (Supplementary Fig. S3A), or UMSCC-1 (Supplementary Fig. S3B) with siRNAs specific for each. Treatment with Bik siRNA resulted in inhibition of carfilzomib- and ONX 0912–induced apoptosis, when compared with treatment with nonspecific siRNA, as assessed by Annexin V staining (Fig. 2C and Supplementary Fig. S3A and S3B) or caspase-3 activation (Fig. 2D). In contrast, siRNA-mediated suppression of Mcl-1 upregulation resulted in enhanced Annexin V staining (Fig. 2C and Supplementary Fig. S3A and S3B) and caspase-3 activation (Fig. 2D) following carfilzomib or ONX 0912 treatment. Taken together, these findings indicate that Bik acts to mediate the pro-apoptotic activities of carfilzomib and ONX 0912 against HNSCCs, whereas upregulated Mcl-1 acts to blunt the killing activities of the compounds.

Carfilzomib and ONX 0912 induce autophagy in HNSCC cells that acts to promote cell survival

We next investigated the impact of carfilzomib and ONX 0912 on cellular autophagy in HNSCCs. Treatment of HNSCCs with carfilzomib or ONX 0912 resulted in upregulation of the autophagy regulatory proteins Beclin-1 and conjugated Atg5/12, suggestive of autophagy induction (Fig. 3A). In addition, both agents markedly induced expression of LC3-II, a processed form of Atg8 (LC3) that is generated during autophagy. In cells undergoing complete autophagic flux, LC3-II is known to be subsequently

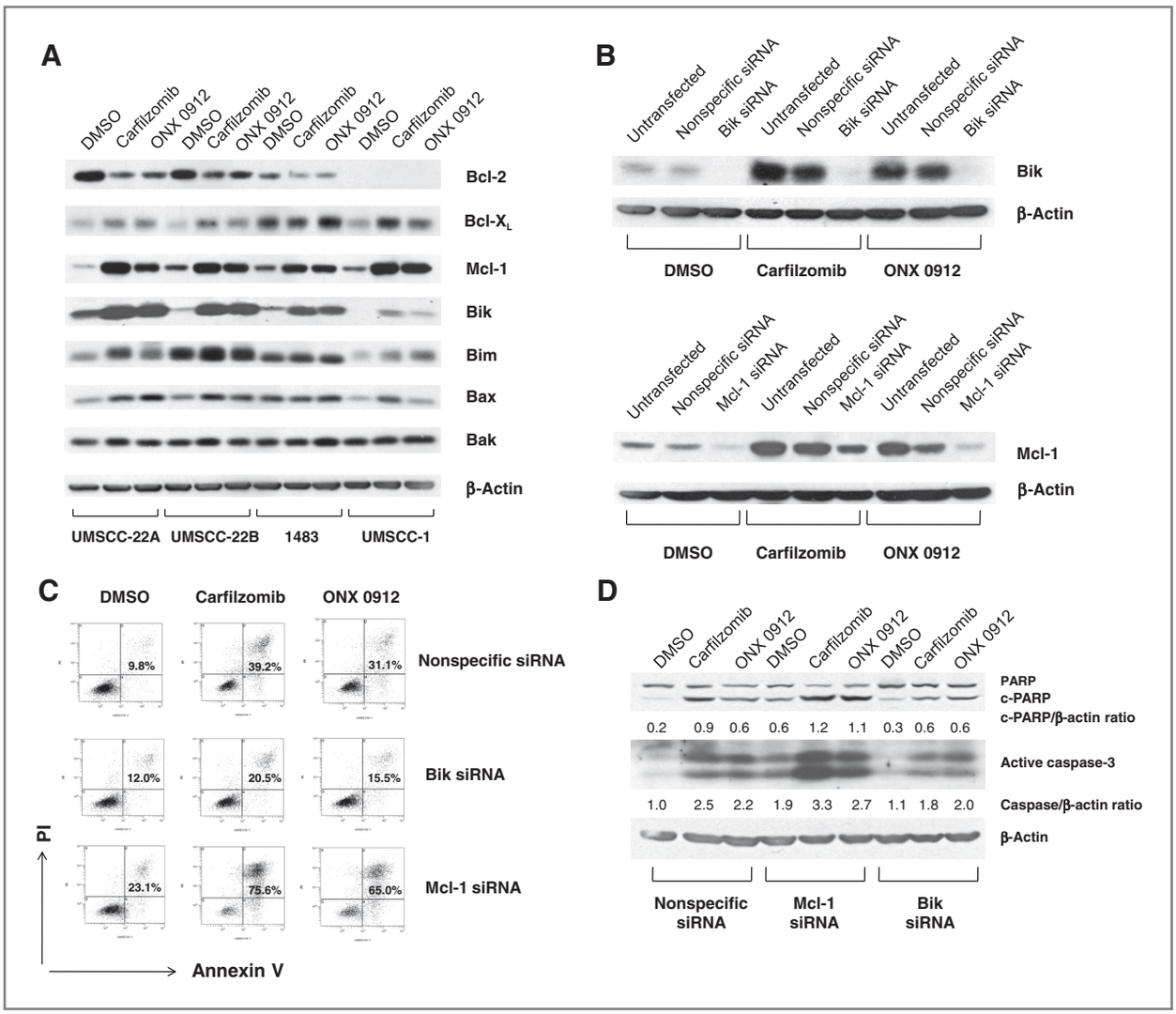

Figure 2. Carfilzomib- and ONX 0912—induced apoptosis is mediated by Bik upregulation, and antagonized by Mcl-1 upregulation. A, UMSCC-22A, UMSCC-22B, 1483, and UMSCC-1 cells were treated for 24 hours with 0.1% DMSO or 100 nmol/L carfilzomib or ONX 0912, followed by immunoblotting for the indicated proteins. In the case of Bik immunoblotting, cells were treated with 200 nmol/L carfilzomib or ONX 0912 to more clearly show Bik upregulation in 1483 and UMSCC-1 cells. Blots shown are representative of 3 independent experiments. B, UMSCC-22A cells were left untreated or were transfected with nonspecific siRNA, Bik siRNA, or Mcl-1 siRNA. Transfected cells were treated for 24 hours with 0.1% DMSO or 100 nmol/L carfilzomib or ONX 0912 and then subjected to immunoblotting for Bik, Mcl-1, or β-actin. C, UMSCC-22A cells transfected with nonspecific, Bik, or Mcl-1 siRNAs were treated for 24 hours with 0.1% DMSO or 100 nmol/L carfilzomib or ONX 0912, followed by flow cytometric analysis of Annexin V/PI staining. Numbers indicate the percentage of Annexin V–positive cells. The experiment was carried out 3 times with similar results. D, UMSCC-22A cells were treated as in B, followed by immunoblotting with anti-PARP, anti-caspase-3, and anti-β-actin. Densitometry was used to calculate ratios. Similar results were seen in 3 independent experiments.

degraded by lysosomal proteases in autolysosomes (34). To determine whether carfilzomib and ONX 0912 induced a complete autophagic flux in HNSCCs, we treated cells with either agent in the absence or presence of the lysosomal protease inhibitors E64d, pepstatin A, and leupeptin (Fig. 3B). Inhibition of lysosomal proteases led to further increases in LC3-II levels in carfilzomib- and ONX 0912–treated cells, indicating that these agents promote complete autophagic flux.

To confirm the induction of autophagy by carfilzomib and ONX 0912, we examined their effects on autophagosome formation (Fig. 3C). UMSCC-22A cells stably expressing GFP-LC3 were treated with carfilzomib and ONX 0912, followed by fluorescence visualization of GFP-LC3-II localization to punctate cytoplasmic dots, an indicator of autophagosome formation (34). Treatment with carfilzomib and ONX 0912 led to a roughly 10-fold increase in the average number of puncta per cell, supporting the conclusion of autophagy induction.

Autophagy induction by bortezomib has been shown to promote either cell death or cell survival, depending on the cell type studied (35–39). To determine whether the

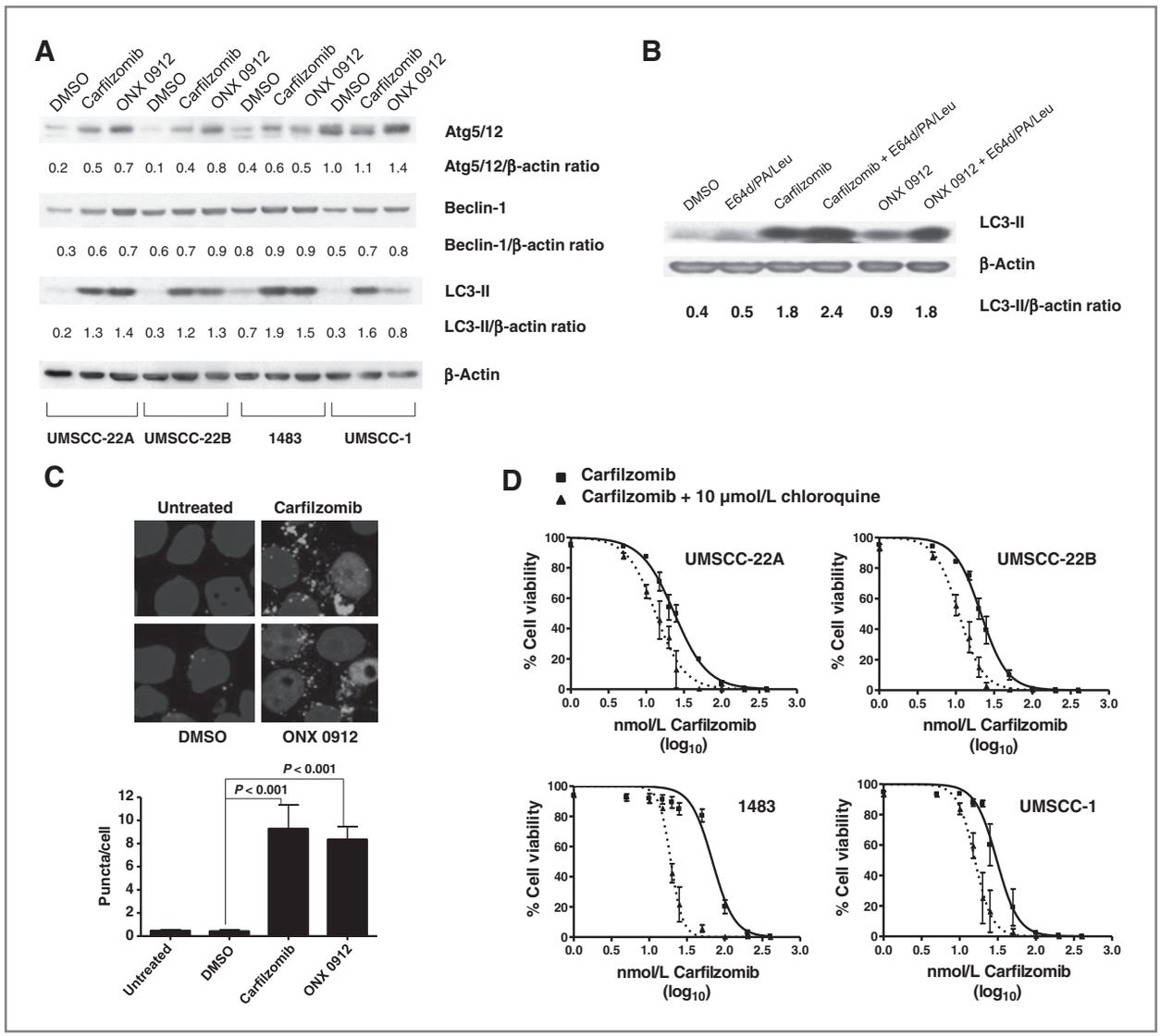

Figure 3. Carfilzomib and ONX 0912 induce prosurvival autophagy in HNSCCs. A, HNSCCs were treated for 24 hours with 100 nmol/L carfilzomib or ONX 0912 or with 0.1% DMSO. Immunoblots were probed for Beclin-1, Atg5/12 conjugate, LC3-II, or β-actin. Representative blots from 3 independent experiments are shown. B, to assess complete autophagic flux, UMSCC-22A cells were treated for 24 hours with 100 nmol/L carfilzomib or ONX 0912 in the absence or presence of the lysosomal protease inhibitors E64d (10 μg/mL), pepstatin A (PA; 10 μg/mL), and leupeptin (Leu; 1 μg/mL). Control cells were treated with DMSO alone or with E64d/PA/Leu alone. Following treatment, cell lysates were probed for LC3-II or β-actin. LC3-II/β-actin ratios were determined by densitometry. Similar results were obtained in 3 independent experiments. C, UMSCC-22A cells stably expressing GFP-LC3 were treated as in A. The treated cells were fixed in paraformaldehyde and nuclei stained with Hoechst 33258. The average number of puncta per cell was determined as described in Materials and Methods. Columns represent the average number of puncta per cell from 3 independent experiments; error bars represent the SEM. D, HNSCCs were treated with the indicated concentrations of carfilzomib in the absence or presence of 10 μmol/L chloroquine. After 48 hours, cell viabilities were determined by trypan blue exclusion assays. Data represent the mean ± SEM from 3 independent experiments.

autophagy induction we observed serves a prodeath or a prosurvival role in HNSCCs, cells were treated with carfilzomib in the absence or presence of the autophagy inhibitor chloroquine, followed by performance of trypan blue exclusion assays (Fig. 3D). Treatment with a subtoxic dose of chloroquine enhanced cell killing by carfilzomib in all 4 HNSCC cell lines examined. A similar trend but reduced magnitude of effect was seen in ONX 0912–treated cells that were cotreated with chloroquine (Supplementary Fig. S5). These findings indicate that autophagy induction promotes cell survival and attenuates the killing activity of carfilzomib and ONX 0912 in HNSCCs.

Carfilzomib and ONX 0912 activation of the UPR leads to ATF4-dependent induction of autophagy

Inhibition of the proteasome leads to cellular accumulation of proteasomal substrate proteins, including unfolded proteins. The accumulation of unfolded proteins is

predicted to activate the UPR, involving phosphorylation/activation of PERK, followed by phosphorylation of eIF2α translation initiation factor and preferential translation of ATF4 transcription factor (40). Prior studies have suggested a role for ATF4 in autophagy induction (41, 42). As shown in Fig. 4A, treatment with carfilzomib or ONX 0912 led to elevated levels of phospho-PERK (p-PERK), phospho-eIF2α (p-eIF2α), and ATF4 in 4 HNSCC cell lines, indicating activation of the UPR.

To determine whether ATF4 upregulation plays a role in carfilzomib- and ONX 0912–induced autophagy, we first conducted a time course analysis of ATF4 and LC3-II expression (Fig. 4B). ATF4 upregulation was first detected at 3 hours in carfilzomib-treated UMSCC-22A cells and at 6 hours in cells treated with ONX 0912, with peak expression occurring 6 or 12 hours after treatment. Upregulation of LC3-II occurred with slower kinetics, with peak levels observed 48 hours after initiation of treatment. To further assess the role of ATF4, we inhibited expression using siRNA (Fig. 4C). Suppression of ATF4 expression resulted in diminished induction of LC3-II in carfilzomib- and ONX 0912–treated UMSCC-22A cells. Highly similar results were seen following knockdown of ATF4 in 1483 (Supplementary Fig. S4A) and UMSCC-1 (Supplementary Fig. S4B) cells. Moreover, a roughly 5-fold reduction in the average number of puncta per cell was observed in carfilzomib- and ONX 0912–treated UMSCC-22A cells that were simultaneously treated with ATF4 siRNA, compared with simultaneous treatment with nonspecific siRNA (Fig. 4D). These findings indicate that upregulation of ATF4 is at least partially responsible for mediating carfilzomib and ONX 0912 induction of autophagy in HNSCCs.

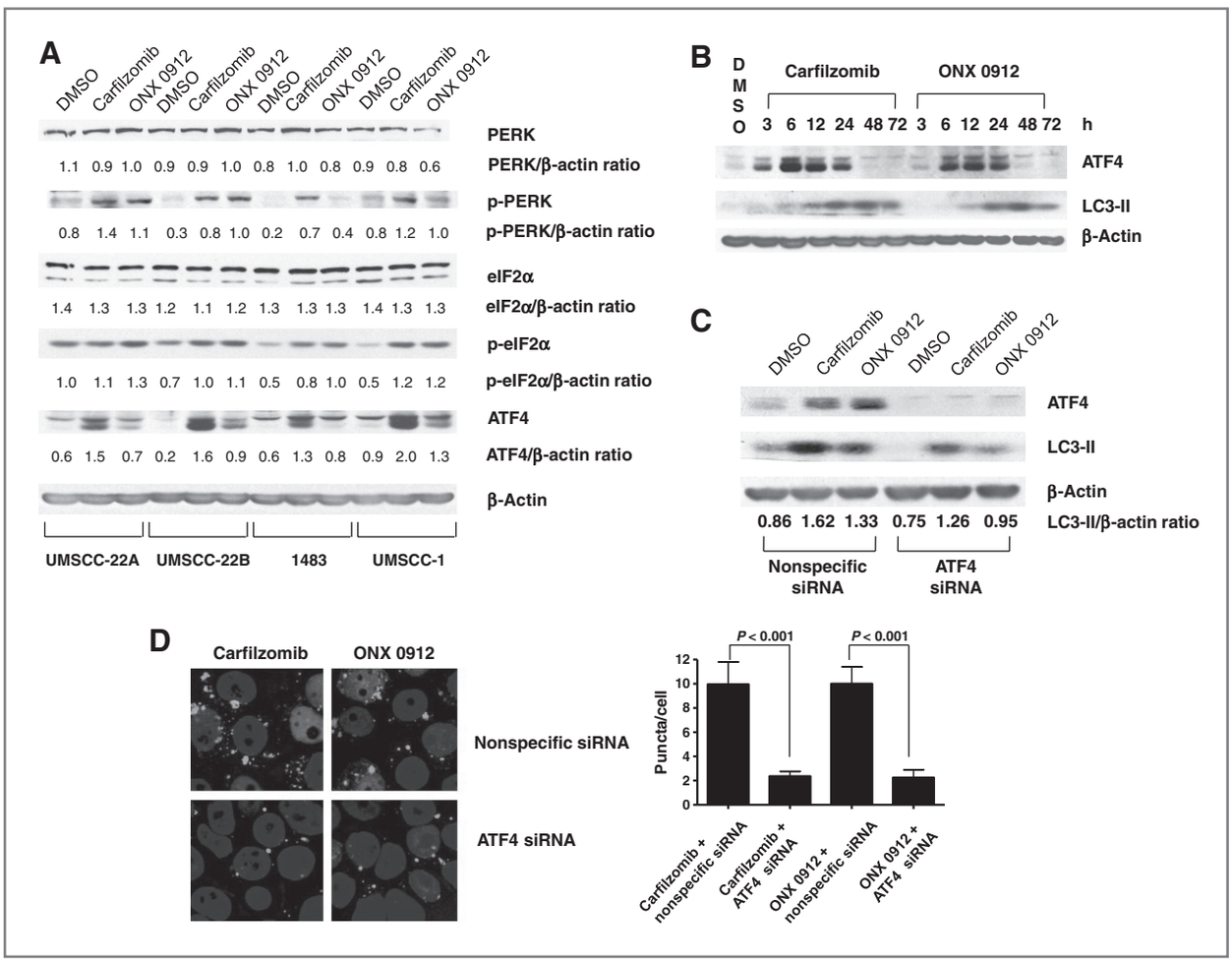

Figure 4. Carfilzomib and ONX 0912 activate the UPR, inducing ATF4-mediated autophagy in HNSCC cells. A, HNSCCs were treated for 24 hours with 0.1% DMSO or 100 nmol/L carfilzomib or ONX 0912. Immunoblotting was used to assess the levels of p-PERK (Ser713), total PERK, p-eIF2α (Ser51), total eIF2α, ATF4, and β-actin. In the case of p-eIF2α and ATF4, immunoblotting was conducted after only 6 hours of treatment. The ratios of immunoblotted proteins to β-actin were determined using β-actin blots from the corresponding time point (6 or 24 hours). Representative blots from 3 independent experiments are shown. B, UMSCC-22A cells were treated for the indicated times with 100 nmol/L carfilzomib or ONX 0912, followed by immunoblotting for ATF4, LC3-II, or β-actin. C, UMSCC-22A cells transfected with nonspecific siRNA or ATF4 siRNA were treated as in A and then subjected to immunoblotting for ATF4, LC3-II, or β-actin. D, UMSCC-22A cells stably expressing GFP-LC3 were transfected with nonspecific siRNA or ATF4 siRNA, followed by treatment for 24 hours with 100 nmol/L carfilzomib or ONX 0912. Columns represent the average number of puncta per cell from 3 independent experiments; error bars represent the SEM.

We next determined the impact of ATF4 suppression on carfilzomib- and ONX 0912–induced apoptosis. Inhibition of ATF4 expression in UMSCC-22A and 1483 cells resulted in a modest enhancement of apoptosis, as assessed by flow cytometric analysis of Annexin V staining (Supplementary Fig. S6A and S6B).

ONX 0912 inhibits HNSCC tumor growth *in vivo*

The antitumor activity of orally administered ONX 0912 was investigated using nude mice harboring HNSCC xenograft tumors. In initial studies,. we sought to determine the impact of ONX 0912 on CT-L activity in the HNSCC tumors. Because ONX 0912 is an irreversible proteasome inhibitor, repeated treatment would be expected to result in cumulative proteasome inhibition. Therefore, a single oral administration of vehicle or ONX 0912 (10 or 30 mg/kg) was given to tumor-bearing mice (3 per group), followed by harvest of tumors or normal tissues 1 hour later (Fig. 5A). In liver tissue, CT-L activity was inhibited by greater than 50% at both doses of ONX 0912, whereas in blood and heart, greater than 50% inhibition was only achieved at the 30 mg/kg dose. In the HNSCC tumors, greater than 50% CT-L inhibition was seen at 30 mg/kg (although only 2 of 3 tumors were evaluable) but not at the lower dose. These findings indicate that a single oral administration of 30 mg/kg effectively inhibited CT-L activity in normal and HNSCC tumor tissues.

We next examined the impact of ONX 0912 on HNSCC tumor growth. Mice harboring HNSCC xenograft tumors (10 per group) were treated with vehicle alone or with ONX 0912 (10 or 30 mg/kg), and tumor volumes were determined (Fig. 5B). Treatments were administered via oral gavage once a day on 2 consecutive days and repeated weekly for 2 weeks. Treatment with 10 mg/kg ONX 0912 did not have a significant effect on tumor growth, relative to treatment with vehicle alone. In contrast, highly significant inhibition of HNSCC tumor growth was seen with 30 mg/kg ONX 0912 ($P = 0.003$). These results show that consecutive-day treatment with orally administered ONX 0912, using a dose that has previously been shown to be well tolerated (22), leads to inhibition of HNSCC tumor growth. In additional *in vivo* studies, we observed dose-dependent antitumor effects of carfilzomib (consecutive-day/once per week, intravenous delivery of 3 or 5 mg/kg carfilzomib; Supplementary Fig. S7).

Discussion

Proteasome inhibition has emerged as a valuable anticancer strategy, particularly in hematologic malignancies. The first-in-class proteasome inhibitor, bortezomib, shows clinical efficacy against myeloma and mantle cell lymphoma and is undergoing evaluation in a variety of other hematologic malignancies. Treatment of solid tumors with bortezomib has met with less success or has not been extensively investigated. In the case of HNSCCs, preclinical studies have shown that bortezomib potently promotes cell death, accompanied by inhibition of NF-κB (26, 30), generation of reactive oxygen species (27), activation of apoptosis and autophagy (27, 28, 33, 43), and suppression of xenograft tumor growth (26). In patients with recurrent HNSCCs, bortezomib in combination with radiation exhibited moderate activity (30, 31). However, a subsequent phase 1 trial involving addition of bortezomib to cetuximab and radiation in HNSCCs was terminated because of unexpected early progression in 5 of 7 patients and advised against bortezomib/cetuximab combination (44).

The application of bortezomib to the treatment of solid tumors has been limited by a number of factors. Because the dipeptide boronate structure of bortezomib acts to reversibly inhibit proteasome activity, prolonged proteasome inhibition requires frequent and extended treatment. Moreover, a high rate of adverse toxicities, including peripheral neuropathy, is seen in bortezomib-treated patients. Recent studies indicate that these adverse events are due to off-target, non-proteasomal effects of bortezomib (16). Bortezomib inhibits both the CT-L and C-L activities of the proteasome and also inhibits the serine proteases chymase, dipeptidyl peptidase II, HtrA2/Omi, and cathepsins A and G. Inherent and acquired resistance to bortezomib represents a further limitation to treatment.

Considerable effort is being invested to develop next-generation proteasome inhibitors that can overcome some of the limitations associated with bortezomib. Carfilzomib is a highly selective inhibitor of the CT-L activity associated with the 20S β5 subunit of the constitutive proteasome that is found in most cells. In addition, carfilzomib inhibits the CT-L activity of the LMP7 subunit of the immunoproteasome that is expressed primarily in hematopoietic cells (18, 20). Carfilzomib does not exhibit inhibitory activity against the multiple serine proteases inhibited by bortezomib, and a markedly reduced rate of peripheral neuropathy has been reported in carfilzomib-treated patients. The epoxyketone moiety of carfilzomib acts to irreversibly inhibit the proteasome, ensuring prolonged inhibition that requires synthesis of new proteasome subunits to restore cellular activity (18). ONX 0912 is a recently derived derivative of carfilzomib that offers the further advantage of being orally bioavailable (22). Both agents inhibit the growth of lymphoma, myeloma, and Waldenstrom macroglobulinemia xenograft tumors (17, 18, 20, 22, 23) and are inhibitory against myeloma cells that are resistant to conventional therapies, including bortezomib (17, 23). A phase 1 study of carfilzomib has shown that it is well-tolerated with consecutive-day dosing (19).

We investigated the activities and mechanisms of carfilzomib and ONX 0912 against HNSCC preclinical models. Both compounds potently promoted cell death in 8 different HNSCC cell lines. ONX 0912 exhibited slightly reduced potency relative to carfilzomib, consistent with findings from the first report of this derivative (22). However, because ONX 0912 offers the unique advantage over carfilzomib and bortezomib of being orally bioavailable, we investigated ONX 0912 antitumor activity *in vivo*. Marked inhibition of CT-L activity in HNSCC xenograft tumors and normal tissues was seen following a single oral

administration of ONX 0912. Furthermore, consecutive-day dosing (on a weekly basis) of 30 mg/kg ONX 0912 yielded potent inhibition of tumor growth, supporting the potential use of this compound in HNSCCs.

Carfilzomib- and ONX 0912–induced cell death was accompanied by activation of apoptosis signaling, mediated, in part, by upregulation of pro-apoptotic Bik. Others have reported that apoptosis induction by carfilzomib, ONX 0912, or other proteasome inhibitors is partially dependent on activation of c-*jun*-NH_2 terminal kinase (JNK) enzymes (17, 20, 45, 46). In HNSCCs, we previously reported that bortezomib-induced JNK activation also acts to promote autophagy (33). The importance of JNK for autophagy induction by carfilzomib and ONX 0912 remains to be determined. We further showed that carfilzomib and ONX 0912 activated the UPR in HNSCC cells,

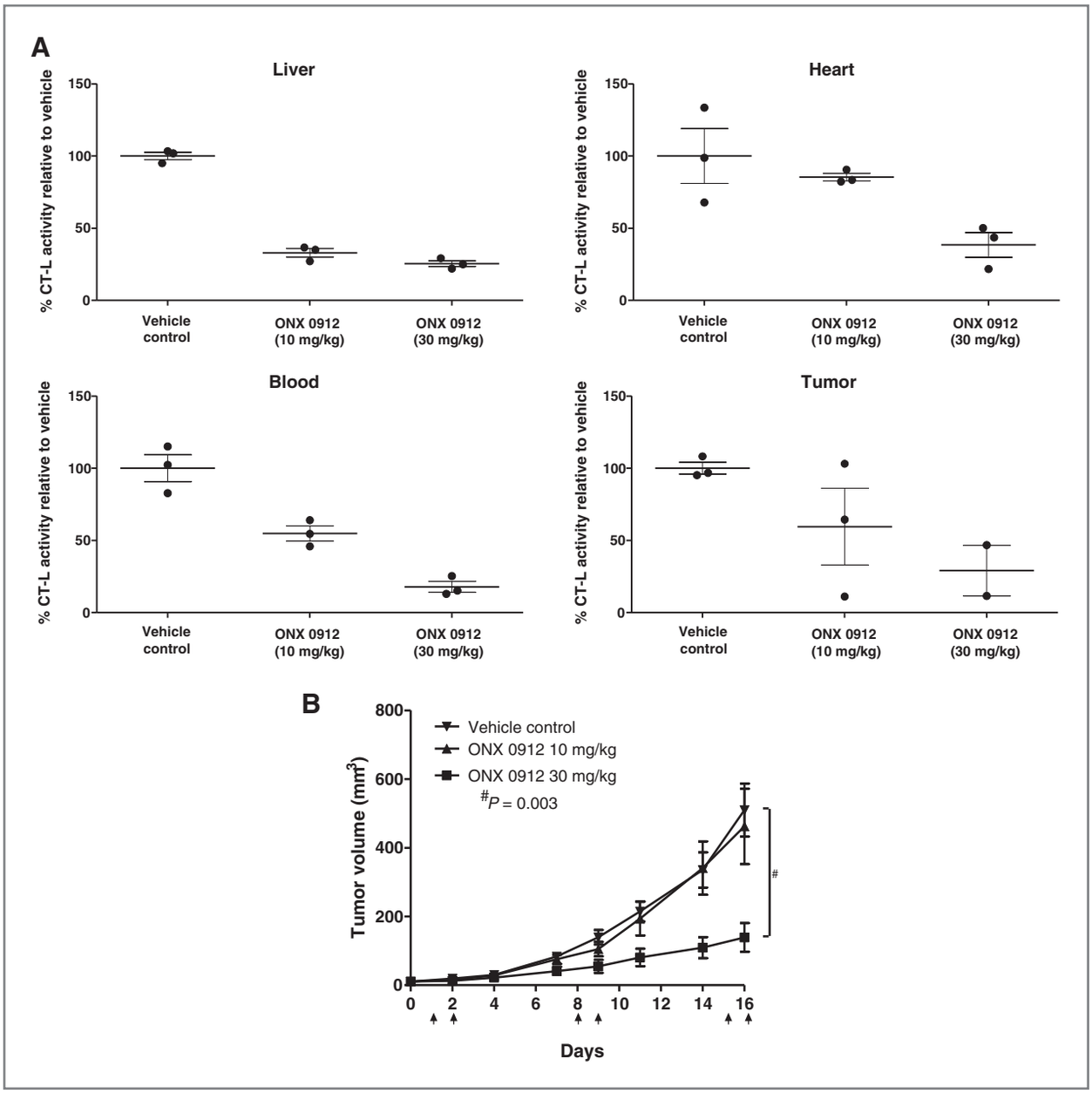

Figure 5. Oral administration of ONX 0912 inhibits HNSCC xenograft tumor growth *in vivo*. A, nude mice bearing HNSCC xenograft tumors were randomized into 3 groups (3 mice per group), followed by a single oral administration of vehicle (1% carboxymethyl cellulose) or ONX 0912 (10 or 30 mg/kg). One hour after treatment, tumors and normal tissues were harvested and CT-L activities were determined. Error bars represent the SEM. B, HNSCC tumor-bearing mice were randomized into 3 groups (10 mice per group) on day 0. Treatment with vehicle or ONX 0912 (10 or 30 mg/kg) was initiated on day 1. Mice were treated once per day for 2 consecutive days and the treatment repeated weekly for 2 weeks (arrows represent treatment days). Mean tumor volumes ± SEM are presented.

leading to induction of ATF4. ATF4 was found to partially mediate autophagy induction by both compounds.

Our studies also revealed 2 approaches that can be pursued for enhancing the killing activities of carfilzomib and ONX 0912 against HNSCCs. Carfilzomib and ONX 0912 were found to upregulate anti-apoptotic Mcl-1 and activate prosurvival autophagy. Suppression of either Mcl-1 or autophagy improved the potencies of carfilzomib and ONX 0912. Thus, combination of carfilzomib or ONX 0912 with inhibitors of Mcl-1 or autophagy may represent a promising therapeutic strategy.

It should be noted that the 8 HNSCC cell lines used in our study do not harbor human papilloma virus (HPV). HPV infection represents an emerging risk factor in HNSCCs and is associated with tumors of the oropharynx and favorable prognosis (47). Notably, in the phase I trial of bortezomib, cetuximab, and radiotherapy in patients with HNSCCs, early termination of the trial occurred when 5 patients with favorable prognosis oropharyngeal cancer progressed within 1 year (44). In contrast, 2 patients, 1 with oropharyngeal cancer and 1 with HPV-negative HNSCC did not exhibit progression. Moreover, *in vitro* studies in HNSCCs and a phase I study in lung cancer and HNSCCs have suggested a benefit of combining bortezomib and EGF receptor (EGFR) inhibitors (29, 48–50). It remains possible that the use of proteasome inhibitors in HPV-positive HNSCCs, where wild-type p53 should be liberated by proteasome inhibition, may lead to alternative outcomes compared with HPV-negative HNSCCs, where p53 is typically mutated or absent. Further studies will be needed to examine the impact and mechanisms of carfilzomib and ONX 0912 in HPV-positive HNSCC models.

In summary, our findings show that carfilzomib and ONX 0912 potently inhibit the viability of HNSCCs *in vitro* and that oral administration of ONX 0912 effectively inhibits growth of HNSCC solid tumors *in vivo*. Our mechanistic studies provide a foundation for enhancing the therapeutic efficacies of carfilzomib and ONX 0912 via cotreatment with inhibitors of anti-apoptotic Mcl-1 protein or autophagy.

Disclosure of Potential Conflicts of Interest

E.T. Chan is employed by Onyx Pharmaceuticals, Inc. as Research Associate and C.J. Kirk as Vice President, Research with Onyx Pharmaceuticals, Inc. C.J. Kirk has ownership interest (including patents) in Onyx Pharmaceuticals, Inc. No potential conflicts of interest were disclosed by the other authors.

Authors' Contributions

Conception and design: Y. Zang, D.E. Johnson
Development of methodology: Y. Zang, S.M. Thomas, C.J. Kirk, D.E. Johnson
Acquisition of data (provided animals, acquired and managed patients, provided facilities, etc.): Y. Zang, S.M. Thomas, E.T. Chan, M.L. Freilino, D. E. Johnson
Analysis and interpretation of data (e.g., statistical analysis, biostatistics, computational analysis): Y. Zang, S.M. Thomas, E.T. Chan, H.M. DeLancey, D.E. Johnson
Writing, review, and/or revision of the manuscript: Y. Zang, S.M. Thomas, C.J. Kirk, H.M. DeLancey, J.R. Grandis, D.E. Johnson
Administrative, technical, or material support (i.e., reporting or organizing data, constructing databases): D.E. Johnson
Study supervision: D.E. Johnson

Acknowledgments

The authors thank Monette Aujay for helpful discussions.

Grant Support

This work was supported by NIH grants R01 CA137260 and P50 CA097190. This project also used UPCI shared resources supported in part by P30CA047904.

The costs of publication of this article were defrayed in part by the payment of page charges. This article must therefore be hereby marked *advertisement* in accordance with 18 U.S.C. Section 1734 solely to indicate this fact.

Received April 12, 2012; revised August 15, 2012; accepted August 15, 2012; published OnlineFirst August 28, 2012.

References

1. Ciechanover A. Proteolysis: from the lysosome to ubiquitin and the proteasome. Nat Rev Mol Cell Biol 2005;6:79–87.
2. Groll M, Ditzel L, Lowe J, Stock D, Bochtler M, Bartunik HD, et al. Structure of 20S proteasome from yeast at 2.4 A resolution. Nature 1997;386:463–71.
3. Orlowski M, Wilk S. Catalytic activities of the 20 S proteasome, a multicatalytic proteinase complex. Arch Biochem Biophys 2000;383:1–16.
4. Rock KL, Gramm C, Rothstein L, Clark K, Stein R, Dick L, et al. Inhibitors of the proteasome block the degradation of most cell proteins and the generation of peptides presented on MHC class I molecules. Cell 1994;78:761–71.
5. Kisselev AF, Callard A, Goldberg AL. Importance of the different proteolytic sites of the proteasome and the efficacy of inhibitors varies with the protein substrate. J Biol Chem 2006;281:8582–90.
6. Bross PF, Kane R, Farrell AT, Abraham S, Benson K, Brower ME, et al. Approval summary for bortezomib for injection in the treatment of multiple myeloma. Clin Cancer Res 2004;10:3954–64.
7. Richardson PG, Barlogie B, Berenson J, Singhal S, Jagannath S, Irwin D, et al. A phase 2 study of bortezomib in relapsed, refractory myeloma. N Engl J Med 2003;348:2609–17.
8. Richardson PG, Sonneveld P, Schuster MW, Irwin D, Stadtmauer EA, Facon T, et al. Bortezomib or high-dose dexamethasone for relapsed multiple myeloma. N Engl J Med 2005;352:2487–98.
9. Fisher RI, Bernstein SH, Kahl BS, Djulbegovic B, Robertson MJ, de Vos S, et al. Multicenter phase II study of bortezomib in patients with relapsed or refractory mantle cell lymphoma. J Clin Oncol 2006;24:4867–74.
10. Orlowski RZ, Nagler A, Sonneveld P, Blade J, Hajek R, Spencer A, et al. Randomized phase III study of pegylated liposomal doxorubicin plus bortezomib compared with bortezomib alone in relapsed or refractory multiple myeloma: combination therapy improves time to progression. J Clin Oncol 2007;25:3892–901.
11. O'Connor OA, Wright J, Moskowitz C, Muzzy J, MacGregor-Cortelli B, Stubblefield M, et al. Phase II clinical experience with the novel proteasome inhibitor bortezomib in patients with indolent non-Hodgkin's lymphoma and mantle cell lymphoma. J Clin Oncol 2005;23:676–84.
12. Richardson PG, Briemberg H, Jagannath S, Wen PY, Barlogie B, Berenson J, et al. Frequency, characteristics, and reversibility of peripheral neuropathy during treatment of advanced multiple myeloma with bortezomib. J Clin Oncol 2006;24:3113–20.
13. Lonial S, Waller EK, Richardson PG, Jagannath S, Orlowski RZ, Giver CR, et al. Risk factors and kinetics of thrombocytopenia associated with bortezomib for relapsed, refractory multiple myeloma. Blood 2005;106:3777–84.

14. Cavaletti G, Jakubowiak AJ. Peripheral neuropathy during bortezomib treatment of multiple myeloma: a review of recent studies. Leuk Lymphoma 2010;51:1178–87.
15. Corso A, Mangiacavalli S, Varettoni M, Pascutto C, Zappasodi P, Lazzarino M. Bortezomib-induced peripheral neuropathy in multiple myeloma: a comparison between previously treated and untreated patients. Leuk Res 2010;34:471–4.
16. Arastu-Kapur S, Anderl JL, Kraus M, Parlati F, Shenk KD, Lee SJ, et al. Nonproteasomal targets of the proteasome inhibitors bortezomib and carfilzomib: a link to clinical adverse events. Clin Cancer Res 2011;17: 2734–43.
17. Kuhn DJ, Chen Q, Voorhees PM, Strader JS, Shenk KD, Sun CM, et al. Potent activity of carfilzomib, a novel, irreversible inhibitor of the ubiquitin-proteasome pathway, against preclinical models of multiple myeloma. Blood 2007;110:3281–90.
18. Demo SD, Kirk CJ, Aujay MA, Buchholz TJ, Dajee M, Ho MN, et al. Antitumor activity of PR-171, a novel irreversible inhibitor of the proteasome. Cancer Res 2007;67:6383–91.
19. O'Connor OA, Stewart AK, Vallone M, Molineaux CJ, Kunkel LA, Gerecitano JF, et al. A phase 1 dose escalation study of the safety and pharmacokinetics of the novel proteasome inhibitor carfilzomib (PR-171) in patients with hematologic malignancies. Clin Cancer Res 2009;15:7085–91.
20. Sacco A, Aujay M, Morgan B, Azab AK, Maiso P, Liu Y, et al. Carfilzomib-dependent selective inhibition of the chymotrypsin-like activity of the proteasome leads to antitumor activity in Waldenstrom's Macroglobulinemia. Clin Cancer Res 2011;17:1753–64.
21. Dasmahapatra G, Lembersky D, Son MP, Attkisson E, Dent P, Fisher RI, et al. Carfilzomib interacts synergistically with histone deacetylase inhibitors in mantle cell lymphoma cells *in vitro* and *in vivo*. Mol Cancer Ther 2011;10:1686–97.
22. Zhou HJ, Aujay MA, Bennett MK, Dajee M, Demo SD, Fang Y, et al. Design and synthesis of an orally bioavailable and selective peptide epoxyketone proteasome inhibitor (PR-047). J Med Chem 2009;52: 3028–38.
23. Chauhan D, Singh AV, Aujay M, Kirk CJ, Bandi M, Ciccarelli B, et al. A novel orally active proteasome inhibitor ONX 0912 triggers *in vitro* and *in vivo* cytotoxicity in multiple myeloma. Blood 2010;116:4906–15.
24. Fung C, Grandis JR. Emerging drugs to treat squamous cell carcinomas of the head and neck. Expert Opin Emerg Drugs 2010;15:355–73.
25. Bonner JA, Harari PM, Giralt J, Cohen RB, Jones CU, Sur RK, et al. Radiotherapy plus cetuximab for locoregionally advanced head and neck cancer: 5-year survival data from a phase 3 randomised trial, and relation between cetuximab-induced rash and survival. Lancet Oncol 2010;11:21–8.
26. Sunwoo JB, Chen Z, Dong G, Yeh N, Crowl Bancroft C, Sausville E, et al. Novel proteasome inhibitor PS-341 inhibits activation of nuclear factor-kappa B, cell survival, tumor growth, and angiogenesis in squamous cell carcinoma. Clin Cancer Res 2001;7:1419–28.
27. Fribley A, Zeng Q, Wang CY. Proteasome inhibitor PS-341 induces apoptosis through induction of endoplasmic reticulum stress-reactive oxygen species in head and neck squamous cell carcinoma cells. Mol Cell Biol 2004;24:9695–704.
28. Li C, Li R, Grandis JR, Johnson DE. Bortezomib induces apoptosis via Bim and Bik up-regulation and synergizes with cisplatin in the killing of head and neck squamous cell carcinoma cells. Mol Cancer Ther 2008;7:1647–55.
29. Lorch JH, Thomas TO, Schmoll HJ. Bortezomib inhibits cell-cell adhesion and cell migration and enhances epidermal growth factor receptor inhibitor-induced cell death in squamous cell cancer. Cancer Res 2007;67:727–34.
30. Van Waes C, Chang AA, Lebowitz PF, Druzgal CH, Chen Z, Elsayed YA, et al. Inhibition of nuclear factor-kappaB and target genes during combined therapy with proteasome inhibitor bortezomib and reirradiation in patients with recurrent head-and-neck squamous cell carcinoma. Int J Radiat Oncol Biol Phys 2005;63:1400–12.
31. Allen C, Saigal K, Nottingham L, Arun P, Chen Z, Van Waes C. Bortezomib-induced apoptosis with limited clinical response is accompanied by inhibition of canonical but not alternative nuclear factor-{kappa}B subunits in head and neck cancer. Clin Cancer Res 2008;14:4175–85.
32. Lin CJ, Grandis JR, Carey TE, Gollin SM, Whiteside TL, Koch WM, et al. Head and neck squamous cell carcinoma cell lines: established models and rationale for selection. Head Neck 2007;29:163–88.
33. Li C, Johnson DE. Bortezomib induces autophagy in head and neck squamous cell carcinoma cells via JNK activation. Cancer Lett 2012;314:102–7.
34. Klionsky DJ, Abeliovich H, Agostinis P, Agrawal DK, Aliev G, Askew DS, et al. Guidelines for the use and interpretation of assays for monitoring autophagy in higher eukaryotes. Autophagy 2008;4: 151–75.
35. Ding WX, Ni HM, Gao W, Yoshimori T, Stolz DB, Ron D, et al. Linking of autophagy to ubiquitin-proteasome system is important for the regulation of endoplasmic reticulum stress and cell viability. Am J Pathol 2007;171:513–24.
36. Zhu K, Dunner K Jr, McConkey DJ. Proteasome inhibitors activate autophagy as a cytoprotective response in human prostate cancer cells. Oncogene 2010;29:451–62.
37. Ding WX, Ni HM, Gao W, Chen X, Kang JH, Stolz DB, et al. Oncogenic transformation confers a selective susceptibility to the combined suppression of the proteasome and autophagy. Mol Cancer Ther 2009;8:2036–45.
38. Hoang B, Benavides A, Shi Y, Frost P, Lichtenstein A. Effect of autophagy on multiple myeloma cell viability. Mol Cancer Ther 2009;8: 1974–84.
39. Belloni D, Veschini L, Foglieni C, Dell'Antonio G, Caligaris-Cappio F, Ferrarini M, et al. Bortezomib induces autophagic death in proliferating human endothelial cells. Exp Cell Res 2010;316:1010–8.
40. Walter P, Ron D. The unfolded protein response: from stress pathway to homeostatic regulation. Science 2011;334:1081–6.
41. Park MA, Curiel DT, Koumenis C, Graf M, Chen CS, Fisher PB, et al. PERK-dependent regulation of HSP70 expression and the regulation of autophagy. Autophagy 2008;4:364–7.
42. Rzymski T, Milani M, Pike L, Buffa F, Mellor HR, Winchester L, et al. Regulation of autophagy by ATF4 in response to severe hypoxia. Oncogene 2010;29:4424–35.
43. Fribley AM, Evenchik B, Zeng Q, Park BK, Guan JY, Zhang H, et al. Proteasome inhibitor PS-341 induces apoptosis in cisplatin-resistant squamous cell carcinoma cells by induction of Noxa. J Biol Chem 2006;281:31440–7.
44. Argiris A, Duffy AG, Kummar S, Simone NL, Arai Y, Kim SW, et al. Early tumor progression associated with enhanced EGFR signaling with bortezomib, cetuximab, and radiotherapy for head and neck cancer. Clin Cancer Res 2011;17:5755–64.
45. Roccaro AM, Sacco A, Aujay M, Ngo HT, Azab AK, Azab F, et al. Selective inhibition of chymotrypsin-like activity of the immunoproteasome and constitutive proteasome in Waldenstrom macroglobulinemia. Blood 2010;115:4051–60.
46. Yang Y, Ikezoe T, Saito T, Kobayashi M, Koeffler HP, Taguchi H. Proteasome inhibitor PS-341 induces growth arrest and apoptosis of non-small cell lung cancer cells via the JNK/c-Jun/AP-1 signaling. Cancer Sci 2004;95:176–80.
47. Chaturvedi AK, Engels EA, Anderson WF, Gillison ML. Incidence trends for human papillomavirus-related and -unrelated oral squamous cell carcinomas in the United States. J Clin Oncol 2008;26:612–9.
48. Dudek AZ, Lesniewski-Kmak K, Shehadeh NJ, Pandey ON, Franklin M, Kratzke RA, et al. Phase I study of bortezomib and cetuximab in patients with solid tumours expressing epidermal growth factor receptor. Br J Cancer 2009;100:1379–84.
49. Wagenblast J, Baghi M, Arnoldner C, Bisdas S, Gstottner W, Ackermann H, et al. Cetuximab enhances the efficacy of bortezomib in squamous cell carcinoma cell lines. J Cancer Res Clin Oncol 2009;135:387–93.
50. Wagenblast J, Baghi M, Arnoldner C, Bisdas S, Gstottner W, Ackermann H, et al. Effect of bortezomib and cetuximab in EGF-stimulated HNSCC. Anticancer Res 2008;28:2239–43.